

# **NOVEL TECHNIQUES TO RAPIDLY DETERMINE THE MAGNETIC ANISOTROPY OF RESERVOIR ROCKS AND SHALES, AND COMPARISONS WITH PERMEABILITY AND ACOUSTIC ANISOTROPIES**

David K. Potter

Department of Physics, and Department of Earth and Atmospheric Sciences,  
University of Alberta, Edmonton, Canada

*This paper was prepared for presentation at the International Symposium of the Society of Core Analysts held in Austin, Texas, USA 18-21 September, 2011*

## **ABSTRACT**

There is a need for rapid, non-destructive methods to determine the anisotropy of reservoir samples and shales in order to rapidly estimate anisotropic petrophysical properties such as permeability anisotropy. Permeability anisotropy measurements themselves are very time consuming as several plugs need to be cut in different orientations to compute an accurate 3D anisotropy ellipsoid, since each plug measurement of permeability is one-dimensional. Moreover, the results are only meaningful if the formation is homogeneously anisotropic on a scale larger than the interval where the plugs are taken. If the formation is heterogeneous at a scale smaller than the plugged interval, then the plugs may have different anisotropies purely due to this heterogeneity as they are cut in slightly different parts of the core. The same issues also apply to acoustic anisotropy if one only makes a one dimensional measurement along the long axis of each plug. Using point transducers, however, one can at least compute the 3D acoustic anisotropy using just 3 core plugs (cut in 3 orthogonal axes) by measuring the acoustic anisotropy in a circular plane in each plug.

This paper will describe a range of rapid, non-destructive low and high field magnetic anisotropy techniques, some of which are new and have not been applied to reservoir samples or shales before. The magnetic techniques only require one plug in order to compute a full 3D anisotropy ellipsoid. The advantages and limitations of the techniques will be discussed. Results using the various magnetic techniques on some tight gas red sandstones and shales are compared to permeability and acoustic anisotropies. An unexpected result is that the maximum acoustic and magnetic axes appeared to correspond to the minimum permeability anisotropy axis in the tight gas red sandstones studied. This might be the result of fine-grained hematite blocking pore connections along the maximum rock framework, and pore network, axis. Another key observation is that high field (rather than low field) anisotropy of magnetic susceptibility (AMS) better reflects the anisotropy of the paramagnetic clays in the shales studied.

## **INTRODUCTION**

Increasingly, there is a need to rapidly estimate the anisotropic properties of core samples, particularly for unconventional reservoirs. Permeability anisotropy is a particularly important parameter and dictates the preferred axis or plane in which fluids will flow in the formation. Anisotropy may also be important for other applications. For instance, a knowledge of the anisotropy of a shale may help one to determine how best to induce fracturing in a shale gas play. Likewise the efficiency of a caprock may in part be governed by the orientation and magnitude of the intrinsic anisotropy.

Determining permeability anisotropy from core samples is a very time consuming and tedious undertaking. Core plug permeability measurements traditionally provide a one-dimensional measurement along the core plug axis, and therefore several core plugs cut in various directions are required to determine the 3D permeability anisotropy. On the other hand magnetic anisotropy methods, or micro-CT imaging, only require a single core plug to determine the 3D anisotropy. These methods, especially the magnetic techniques, are very rapid. A major objective of this research is to compare the various anisotropy techniques with the ultimate aim of potentially estimating permeability anisotropy, for example, from rapid, non-destructive magnetic techniques, since bulk magnetic susceptibility and permeability can be related (Potter, 2007). The present paper will detail the various current and potential anisotropy methods, in particular magnetic anisotropy methods. The advantages and limitations of each method will be discussed. The paper will then show some preliminary results from tight gas sandstone samples, and some shale samples, and will demonstrate how the magnetic anisotropy methods provide valuable insights into the anisotropic properties of other petrophysical parameters.

## **METHODS**

Table 1 summarises various petrophysical anisotropy techniques together with current and proposed magnetic anisotropy methods. The equipment required, typical timescales for measurement, advantages and limitations are listed. The various methods are described in more detail below.

### **Permeability Anisotropy**

Permeability anisotropy measurements are very time consuming as several plugs (at least 9, and preferably 18) need to be cut in different orientations to compute the 3D anisotropy. Each plug measurement of permeability anisotropy is one-dimensional. Furthermore, the results are only meaningful if the formation is homogeneously anisotropic on a scale larger than the interval where the plugs have been taken. If the formation is heterogeneous on a scale smaller than the interval where the plugs have been taken, then the plugs may have different anisotropies merely due to this heterogeneity, since they are cut in slightly different parts of the core section.

### **Acoustic Anisotropy**

The same issues also apply to acoustic anisotropy. However, one can also compute 3D acoustic anisotropy using just 3 core plugs (oriented in 3 orthogonal axes) by measuring

the acoustic anisotropy in 3 circular planes (each circular cross-section of the 3 cylindrical core plugs) using point transducers. This is still quite time consuming and often not very sensitive. Acoustic anisotropy measurements can usually be made with an accuracy of just a few percent.

### **Anisotropy from Imaging Techniques**

Micro-computer tomography (CT) anisotropic imaging (Nasseri *et al*, 2011) of small core plugs is becoming an increasingly important tool, and anisotropic property prediction is starting to become a reality. A major advantage of this imaging is that the anisotropy can be predicted from just one core plug. Most of these studies, however, look at very small sample volumes. However, Clavaud *et al* (2008) have studied larger samples using X-ray tomography. Charpentier *et al* (2003) looked at backscattered scanning electron microscope images (BSEM) of the alignment of clays in small samples of mudstones. This provided important evidence that the anisotropy was related to illitization of smectite and not just depth and effective stress.

### **Magnetic Anisotropy**

#### 1. Low field anisotropy of magnetic susceptibility (AMS)

Low field AMS only requires 1 plug in order to compute a complete 3D anisotropy ellipsoid. A low field anisotropy of magnetic susceptibility (AMS) measurement can be done in just 1 minute. This technique is very common in rock magnetic and palaeomagnetic studies and various measurement schemes and equipment have been described in detail (Girdler, 1961; Collinson, 1983; Tarling and Hrouda, 1993; Borradaile and Stupavsky, 1995). The technique is very sensitive and can measure anisotropies to about 1 part in 10,000, which is substantially better than permeability anisotropy or acoustic anisotropy. It can identify extremely small anisotropies within the bedding plane, which may be related to fluid pathways, and which acoustic and permeability anisotropy measurements are not capable of detecting. A study in mudstones identified correspondences between low field AMS and the amount of illite in the sample (Potter and Ivakhnenko, 2008). Vishnu *et al* (2010) have recently compared low field AMS with *p*-wave velocity in quartzites. The AMS technique gives the sum of the anisotropies of all the mineral components in the sample, so anisotropies due to different mineral components cannot be separated. Another limitation is that AMS is dependent upon ferrimagnetic particle size. Uniaxial stable single-domain particles have a minimum magnetic susceptibility along their long axis, whereas similar larger multidomain particles have a maximum magnetic susceptibility along their long axis (Stephenson *et al*, 1986; Potter and Stephenson, 1988; Rochette, 1988; Rochette *et al*, 1992; Ferre, 2002).

#### 2. Low field AMS after ferrifluid injection

Pfleiderer and Halls (1994) first suggested a technique involving injecting reservoir rocks with a ferrifluid (a water based or oil based fluid containing high magnetic susceptibility ferrimagnetic superparamagnetic nanometre sized particles) to try to estimate the anisotropy of the pore space. The ferrifluid improves the signal to noise ratio since the magnetic susceptibility of most clean sandstones is relatively low due to the

predominance of diamagnetic quartz. However, the theoretical mechanism behind the method is poorly understood. Perfectly dispersed superparamagnetic particles in a fluid ought to produce no AMS, unless of course some of the particles stick to the sides of the pores and throats.

### 3. High field AMS

High field AMS techniques are far less common, and very little work has been reported on the methodologies or their application to petrophysics. High field AMS uniquely allows one to separate out the anisotropy of the paramagnetic (*e.g.*, illite clay) plus diamagnetic (*e.g.*, quartz) components from the ferrimagnetic components (Martin-Hernandez and Ferre, 2007) and thus, for example, more accurately quantify the anisotropy of paramagnetic permeability controlling clays. We have been developing two novel potential methodologies for determining high field AMS. One method is to take high field torque curves in 3 orthogonal sample directions and use a least squares type fit to calculate the anisotropy. Another method involves taking a series of magnetic hysteresis measurements using a Variable Field Translation Balance (VFTB, see Figure 1), with the field applied in a different sample direction for each hysteresis curve. Isotropic samples show no difference in the high field hysteresis curves, whereas anisotropic samples exhibit differences which can be used to estimate the anisotropy.

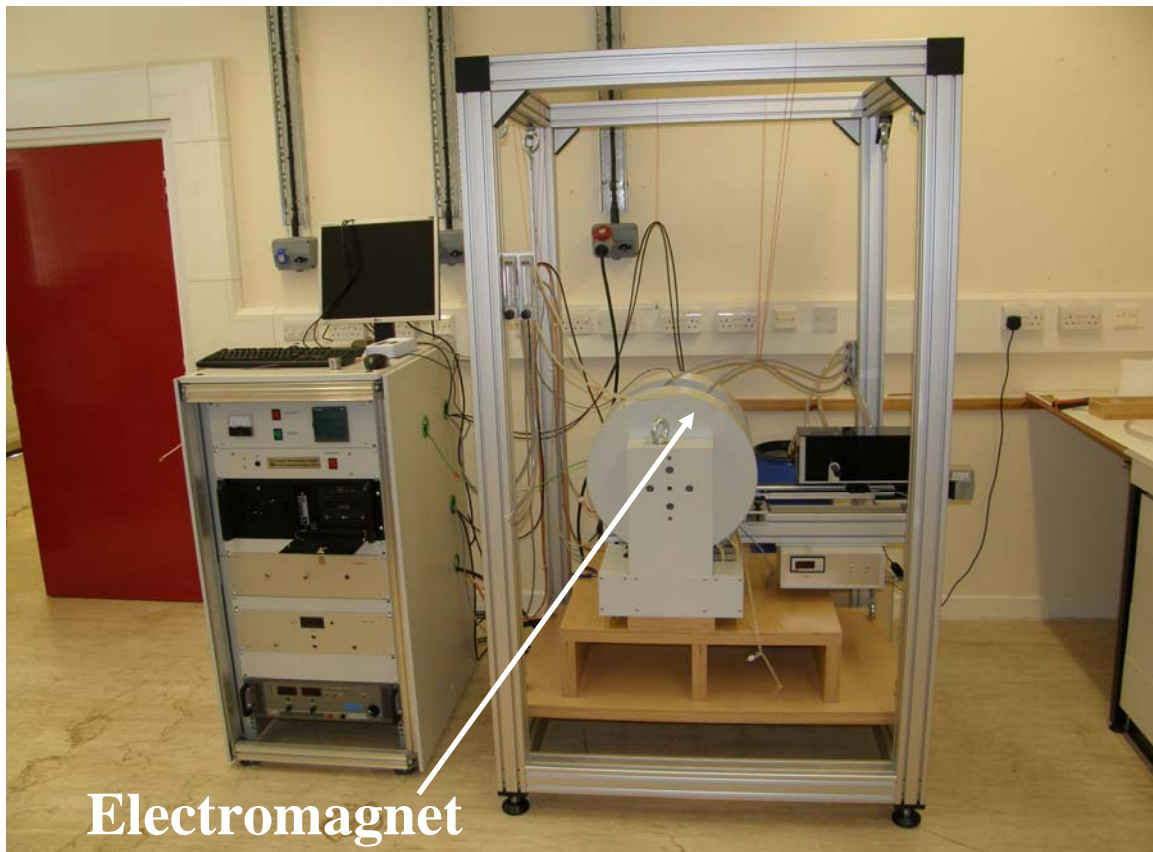


**Figure 1.** Variable Field Translation Balance, which can potentially be used for high field AMS studies.

**Table 1.** A summary comparison of different petrophysical anisotropy techniques.

<b>ANISOTROPY METHOD</b>	<b>EQUIPMENT AND TIME</b>	<b>ADVANTAGES</b>	<b>LIMITATIONS</b>
<b>Permeability Anisotropy</b>	Plug permeameter. Several hours or days.	Direct measurements of permeability.	Requires several plugs. Assumes all plugs have similar homogeneous anisotropy.
<b>Acoustic Anisotropy</b>	Acoustic source, receiver and ideally point transducers. Several minutes or hours.	Direct measurements of <i>p</i> - and <i>s</i> -wave transit times.	Requires at least 3 orthogonal plugs. Assumes all plugs have similar homogeneous anisotropy.
<b>Anisotropy via image analysis</b>	Micro-CT. Several minutes or hours.	Only requires one plug.	The plug size is relatively small. Requires specialized equipment.
<b>Magnetic Anisotropy:</b>			
1. Low field Anisotropy of Magnetic Susceptibility (AMS)	AMS delineator and bulk susceptibility bridge. About 1 minute.	Only requires one plug to get a full 3-D anisotropy ellipsoid. Rapid, sensitive.	Gives the combined sum of all the minerals present, including any ferrimagnetics.
2. Ferrifluid injection followed by low field AMS	AMS delineator and bulk susceptibility bridge. Several hours for ferrifluid injection, and 1 minute for measurement.	Thought to represent the pore anisotropy.	Theoretical mechanism is poorly understood.
3. High field AMS	High field torquemeter or VFTB. Several minutes to a few hours.	Identifies the anisotropy of the diamagnetic plus paramagnetic minerals from the ferrimagnetic ones.	Requires specialized, expensive equipment.
4. Anisotropy of Magnetic Remanence (AMR)	Pulse magnetizer and magnetometer for Anisotropy of Isothermal Remanent Magnetization (AIRM). About 20 minutes. Other AMR techniques take longer.	Only measures the anisotropy of the remanence carrying particles. Rapid. Only requires one plug. Large signal even for low concentrations.	Requires specialised equipment.

#### 4. Anisotropy of Magnetic Remanence (AMR)

Anisotropy of magnetic remanence (AMR) methods allow one to uniquely characterise the anisotropy of the remanence carrying mineral distributions, generally iron oxides, in reservoir samples. These iron oxides can block pores and influence permeability (Potter et al, 2009) and thus their anisotropic distribution might show some correspondence with permeability anisotropy. Anisotropy of isothermal remanent magnetization (AIRM) is likely to be the most useful remanence anisotropy method since isothermal remanence gives the largest signal of any of the remanence methods (Potter, 2004). The methodology involves applying an appropriate direct field (DF) successively along the x, y, and z sample reference axes (x, y and z are orthogonal to one another) and measuring the three components of remanence acquired after each field treatment ( $M_{1x}$ ,  $M_{1y}$ ,  $M_{1z}$  after a field applied along x *etc*). For AIRM this involves applying a pulsed DF, which was made using a Molspin pulse magnetizer. The pulse is very rapid (about 100 ms). The procedure gives nine components of remanence as shown in Equation (1) below: a single estimate of each diagonal tensor element, and two estimates for each pair of corresponding off-diagonal terms.

<u>Field Axis</u>	<u>Measured Remanence</u>	
x	$M_{1x} \ M_{1y} \ M_{1z}$	
y	$M_{2x} \ M_{2y} \ M_{2z}$	(1)
z	$M_{3x} \ M_{3y} \ M_{3z}$	

Each pair of off-diagonal terms is averaged thus giving 3 off-diagonal coefficients, which, together with the 3 diagonal coefficients, are then used to compute a 3-D remanence anisotropy ellipsoid (Potter, 2004) comprising the magnitude and direction of the three principal anisotropy axes (max, int, min). The sample is tumble AF demagnetized between each field application, and any residual remanence components are subtracted from the subsequent laboratory remanence that is imparted.

Other AMR techniques have been described by McCabe et al (1985), Jackson (1991) and Potter (2004). Another advantage of AMR techniques is that they are not dependent upon the domain state of the remanence carrying particles (unlike AMS). Single domain and multidomain particles all have a maximum remanence along their long axis (Stephenson et al, 1986; Potter and Stephenson, 1988).

## **RESULTS**

### **Tight gas red sandstone samples**

Table 2 shows the principal anisotropy axes for some tight gas red sandstone samples from various methods in visually homogenous intervals. For each “sample” air permeability anisotropy and acoustic anisotropy were derived from 18 core plugs oriented in different directions. High field AMS was determined from one core plug from magnetic hysteresis curves using a VFTB (Ivakhnenko and Potter, 2008) successively from 18 orientations of the applied field. AMR was determined on one core plug via 3 applications of a pulse DF as described above.

**Table 2.** Principal anisotropy axes for tight gas red sandstone samples from different anisotropy methods.

## (a) Red sandstone sample RSG12

Method	Principal Axes	Normalised Magnitudes	Directions	
			Dec	Inc
Permeability Anisotropy	max	0.369	82	-10
	int	0.328	51	74
	min	0.303	353	-12
Acoustic Anisotropy ( <i>p</i> -wave velocity)	max	0.345	4	-9
	int	0.331	48	72
	min	0.324	85	-15
High field AMS	max	0.340	359	-7
	int	0.332	54	77
	min	0.328	93	-6
AMR (AIRM 60 mT)	max	0.351	357	-13
	int	0.333	46	71
	min	0.321	91	-14

## (b) Red sandstone sample RSG17

Method	Principal Axes	Normalised Magnitudes	Directions	
			Dec	Inc
Permeability Anisotropy	max	0.374	96	3
	int	0.332	310	85
	min	0.294	4	-3
Acoustic Anisotropy ( <i>p</i> -wave velocity)	max	0.344	5	-4
	int	0.334	303	86
	min	0.322	87	1
High field AMS	max	0.341	357	-2
	int	0.334	328	83
	min	0.325	94	4
AMR (AIRM 60 mT)	max	0.349	358	-6
	int	0.335	344	84
	min	0.316	89	1

**Table 3.** Principal anisotropy axes for shale samples from different anisotropy methods.

## (a) Shale sample GTS1

Method	Principal Axes	Normalised Magnitudes	Directions	
			Dec	Inc
Acoustic Anisotropy ( <i>p</i> -wave velocity)	max	0.350	52	-2
	int	0.344	322	1
	min	0.306	245	-87
Low field AMS	max	0.344	32.2	-0.8
	int	0.339	301.9	-15.3
	min	0.317	125.1	-74.7
High field AMS	max	0.348	49	-4
	int	0.343	315	2
	min	0.309	232	-85
AMR (AIRM 60 mT)	max	0.358	34	-1
	int	0.349	294	-17
	min	0.293	119	-72

## (a) Shale sample GTS2

Method	Principal Axes	Normalised Magnitudes	Directions	
			Dec	Inc
Acoustic Anisotropy ( <i>p</i> -wave velocity)	max	0.354	6	-4
	int	0.350	276	2
	min	0.295	207	-85
Low field AMS	max	0.342	4.5	-12.4
	int	0.341	274.6	0.7
	min	0.317	188.0	-77.6
High field AMS	max	0.350	8	-3
	int	0.347	283	1
	min	0.303	212	-86
AMR (AIRM 60 mT)	max	0.355	6	-14
	int	0.348	281	2
	min	0.297	173	-74

Interestingly, the maximum acoustic, high field AMS and AMR axes seem to correspond to the minimum permeability axis for these samples. The reason for this is not clear at present. The AMR signal is due mainly to fine-grained hematite particles. Perhaps if the hematite particles are preferentially aligned along the maximum rock framework, and pore network, axis (the AMR, high field AMS and acoustic results would be consistent with this), they might preferentially block the pore connections along that axis, causing the permeability to be a minimum in that axis. The results may add weight to suggestions that these hematite particles are an important control on permeability in these samples, compared to white sandstone samples (containing no hematite) in the same reservoir (Potter et al, 2009). This previous work demonstrated that permeability was always lower in the red sandstone intervals compared to adjacent white sandstone intervals.

### **Shale samples**

Table 3 shows the principal anisotropy axes for some shale samples determined from various anisotropy methods in a homogenous interval. For these samples tests using a probe permeameter suggested that the permeability was too low to get accurate results from plug measurements using our equipment, and so permeability anisotropy was not determined. For each “sample” the acoustic anisotropy was this time derived from 3 orthogonal plugs and measurements around the circular cross-section of each plug using point transducers. Low field AMS was determined on one core plug using a Molspin anisotropy delineator in conjunction with a Molspin bulk susceptibility bridge. High field AMS was determined from one core plug from magnetic hysteresis curves successively made from 18 orientations of the applied field. AMR was determined on one core plug via 3 applications of a pulse DF as described above.

All the methods indicate a planar fabric where the maximum and intermediate axes are close in magnitude. Significantly, the orientation of the high field AMS principal axes are closer to the acoustic values than the low field AMS values. This is most likely due to the fact that the high field AMS results reflect the preferred orientation of the paramagnetic clays (the main component in these shales). On the other hand the low field AMS results can be influenced by very small amounts of ferrimagnetic particles, which do not significantly influence the high field AMS results (since these ferrimagnetic particles have saturated at high field) or the acoustic results (since the ferrimagnetic particles generally comprise an extremely small volume of the sample). This seems to be supported by the fact that the orientation of the low field AMS principal axes are more like the AMR values (which are governed exclusively by the remanence carrying, generally ferrimagnetic, particles).

## **CONCLUSIONS**

The main conclusions from this work can be summarised as follows:

- Results on some tight gas red sandstones showed that the maximum acoustic, high field AMS and AMR axes appeared to correspond to the minimum permeability axis. The reason for this is not clear at present. One possibility is that fine-grained

hematite particles are preferentially aligned along the maximum rock framework, and pore network, axis (the acoustic, high field AMS and AMR results would be consistent with this) and are preferentially blocking pore connections causing the permeability to be lower in this axis.

- High field AMS appears to more accurately describe the anisotropy of the paramagnetic clay minerals (compared to low field AMS) in the shales studied, since the high field results were not influenced by the ferrimagnetic mineral fraction that contributes to the low field AMS signal.
- Low and high field AMS measurements, along with AMR measurements, provide very rapid, non-destructive techniques for separating anisotropies due to different mineral fractions (for example, paramagnetic clays versus ferrimagnetic iron oxides) in shales.
- An understanding of the relationship between the magnitude of the magnetic, acoustic and permeability anisotropy may ultimately allow one to make rapid estimates of the magnitude of the permeability and acoustic anisotropy from the magnetic anisotropy measurements.

## ACKNOWLEDGEMENTS

The support of Imperial Oil, who funded part of this work through their University Research Award program, is gratefully acknowledged. The support of an NSERC Discovery Grant is also gratefully acknowledged.

## REFERENCES

- Borradaile, G. J. and Stupavsky, M., 1995. Anisotropy of magnetic susceptibility – measurement schemes. *Geophysical Research Letters*, **22**, 1957-1960.
- Charpentier, D., Worden, R. H., Dillon, C. G. and Aplin, A. C., 2003. Fabric development and the smectite to illite transition in Gulf of Mexico mudstones: an image analysis approach. *J. Geochem. Exploration*, **78-9**, 459-463.
- Clavaud, J. B., Mainault, A., Zamora, M., Rasolofosaon, P., and Schlitter, C., 2008. Permeability anisotropy and its relations with porous medium structure. *J. Geophys. Res. – Solid Earth*, **113**, B01202.
- Collinson, D. W. 1983. *Methods in Rock Magnetism and Palaeomagnetism*. Chapman and Hall, London, pp.503.
- Ferre, E. C., 2002. Theoretical models of intermediate and inverse AMS fabrics. *Geophysical Research Letters*, **29**, art. no. 1127.
- Girdler, R. W., 1961. The measurement and computation of anisotropy of magnetic susceptibility in rocks. *Geophysical Journal of the Royal Astronomical Society*, **5**, 34-44.

Ivakhnenko, O. P. and Potter, D. K., 2008. The use of magnetic hysteresis and remanence measurements for rapidly and non-destructively characterizing reservoir rocks and fluids. *Petrophysics*, **49**, (issue 1), 47-56.

Jackson, M., J. 1991. Anisotropy of magnetic remanence – a brief review of mineralogical sources, physical origins, and geological applications, and comparison with susceptibility anisotropy. *Pure and Applied Geophysics*, **136**, 1-28.

McCabe, C., Jackson, M., Ellwood, B. B., 1985. Magnetic anisotropy in the Trenton Limestone: results of a new technique, anisotropy of anhysteretic susceptibility. *Geophysical Research Letters*, **12**, 333-336.

Martin-Hernandez, F. and Ferre, E. C., 2007. Separation of paramagnetic and ferromagnetic anisotropies: a review. *J. Geophys. Res. – Solid Earth*, **112**, Issue B3, Article no. B03105.

Nasseri, M. H. B., Rezanezhad F. and Young R. P., 2011. Analysis of fracture damage zone in anisotropic granitic rock using 3D X-ray scanning techniques. *International Journal of Fracture*, **168**, 1-13.

Pfleiderer, S. and Halls, H. C., 1994. Magnetic pore fabric analysis – a rapid method for estimating permeability anisotropy. *Geophys. J. Int.*, **116**, 39-45.

Potter, D. K., 2004. A comparison of anisotropy of magnetic remanence methods: a users guide for application to palaeomagnetism and magnetic fabric studies. In “Magnetic Fabric: Methods and Applications.” Martin-Hernandez, F., Luneburg, C. M., Aubourg, C. and Jackson, M. (eds.), *Geological Society, London, Special Publications*, **238**, 21-35.

Potter, D. K., 2007. Magnetic susceptibility as a rapid, non-destructive technique for improved petrophysical parameter prediction. *Petrophysics*, **48**, (issue 3), 191-201.

Potter, D. K and Ivakhnenko, O. P., 2008. Clay typing - sensitive quantification and anisotropy in synthetic and natural reservoir samples using low- and high-field magnetic susceptibility for improved petrophysical appraisals. *Petrophysics*, **49**, (issue 1), 57-66.

Potter, D. K. and Stephenson, A. 1988. Single-domain particles in rocks and magnetic fabric analysis. *Geophysical Research Letters*, **15**, 1097-1100.

Potter, D. K., Ali, A. and Ivakhnenko, O. P., 2009. Quantifying the relative roles of illite and hematite on permeability in red and white sandstones using low and high field magnetic susceptibility. *2009 International Symposium of the Society of Core Analysts*, Noordwijk aan Zee, The Netherlands. Paper SCA2009-11.

Rochette, P. 1988. Inverse magnetic fabric in carbonate-bearing rocks. *Earth and Planetary Science Letters*, **90**, 229-237.

Rochette, P., Jackson, M. J., and Aubourg, C. 1992. Rock magnetism and the interpretation of anisotropy of magnetic susceptibility. *Reviews of Geophysics*, **30**, 209-226.

Stephenson, A., Sadikun, S. and Potter, D. K. 1986. A theoretical and experimental comparison of the anisotropies of magnetic susceptibility and remanence in rocks and minerals. *Geophysical Journal of the Royal Astronomical Society*, **84**, 185-200.

Tarling, D. H. and Hrouda, F. 1993. *The Magnetic Anisotropy of Rocks*. Chapman and Hall, pp.217.

Vishnu, C., Mamtani, M. and Basu, A., 2010. AMS, ultrasonic *p*-wave velocity and rock strength analysis in quartzites devoid of mesoscopic foliations – implications for rock mechanics studies. *Tectonophysics*, **494**, 191-200.